Absorption Characteristics of a Metasurface composed of Gallium Nitride Coated Spherical Inclusions

Hamza Basharat

Department of Electronics

Quaid-i-Azam University, Islamabad, Pakistan

A Thesis Submitted in Partial Fulfillment of the Requirements for the Degree of

Master of Philosophy in Electronics

August, 2023

DEPARTMENT OF ELECTRONICS
QUAID-I-AZAM UNIVERSITY
ISLAMABAD, PAKISTAN

A thesis entitled *Absorption Characteristics of a Metasurface composed of Gallium Nitride Coated Spherical Inclusions* by Hamza Basharat in partial fulfilment of the requirements for the degree of Master of Philosophy, has been approved and accepted by the following,

---

Supervisor
Dr. Muhammad Arshad Fiaz
Associate Professor
Department of Electronics
Quaid-i-Aazam University
Islamabad, Pakistan

Chairman
Prof. Dr. Qaisar Abbas Naqvi
Professor
Department of Electronics
Quaid-i-Aazam University
Islamabad, Pakistan

بِسْمِ اللَّهِ الرَّحْمَٰنِ الرَّحِيمِ

إِنَّ فِي خَلْقِ السَّمَاوَاتِ وَالْأَرْضِ وَاخْتِلَافِ اللَّيْلِ وَالنَّهَارِ وَالْفُلْكِ الَّتِي تَجْرِي فِي الْبَحْرِ بِمَا يَنفَعُ
النَّاسَ وَمَا أَنزَلَ اللَّهُ مِنَ السَّمَاءِ مِن مَّاءٍ فَأَحْيَا بِهِ الْأَرْضَ بَعْدَ مَوْتِهَا وَبَثَّ فِيهَا مِن كُلِّ
دَابَّةٍ وَتَصْرِيفِ الرِّيَاحِ وَالسَّحَابِ الْمُسَخَّرِ بَيْنَ السَّمَاءِ وَالْأَرْضِ لَآيَاتٍ لِّقَوْمٍ يَعْقِلُونَ ○
(البَقَرَة : 164)

Verily, in the creation of the heavens and the earth, and in the alternation of the night and the day, and in the ships (and vessels) which sail through the ocean carrying cargo profitable for the people, and in the (rain) water which Allah pours down from the sky, reviving therewith the earth to life after its death, and (the earth) in which He has scattered animals of all kinds, and in the changing wind directions, and in the clouds (that trail) between the sky and the earth, duty-bound certainly, (in these) are (many) signs for those who put their reason to work.

(Al-Baqarah : 164)

Affectionately dedicated to Shagufta Basharat and Basharat Ali, the two pillars of my life.

Acknowledgements

I humbly extend my gratitude to the Almighty Allah and His last Prophet Muhammad (S.A.W.W), whose strength has empowered me to achieve this milestone. My sincere appreciation goes to Dr. Muhammad Arshad Fiaz, my supervisor, for His unwavering patience, guidance, and support. His extensive knowledge has been an invaluable resource for me. I am profoundly thankful for His mentorship and belief in me throughout my journey.

I thank my university "Quaid I Azam University, Islamabad" who provided a competitive platform to show my skills. Above all, how can I forget our parents? I would like to thank my parents for struggling for me and bringing me up on this stage. Without their tireless efforts and prayers, I would not be able to be at this stage of life.

Lastly, My gratitude extends to all those who have directly and indirectly supported me throughout this transformative journey.

Hamza Basharat
September 1, 2023

Abstract

A comprehensive research has been done to analyze the magnitude of reflection coefficients from a metasurface composed of Gallium-Nitride coated spherical particles under oblique incidence. The material considered for coating is Gallium Nitride. To make the problem simpler, the incident wave is taken to be normal, and a metasurface (MS) is placed in a free-space background. By changing the thickness of the coating material on the sphere's surface, one can adjust the amount of absorption. In this work, the magnitude of thereflection coefficient versus the relative permeability of uncoated and coated magneto-dielectric spheres has been studied. In this study, it has been observed that Gallium- Nitride coated magneto dielectric surface placed in a metasurface with free space as background acts as a good reflector.

Contents

Contents vi

List of Figures viii

Abbreviations ix

1 Introduction 1

1.1 **Layout** 6

1.1.1 Chapter 2 6

1.1.2 Chapter 3 6

1.1.3 Chapter 4 6

1.1.4 Chapter 5 6

2 Geometry and Derivation of Absorption Characteristics for a Metasurface Comprising Coated (GaN) Spherical Inclusions 7

2.1 Mathematical Derivation 8

2.1.1 Uncoated Spherical Scatters..13

2.1.2 Coated Spherical Scatters...15

3 Analysis of Absorption Characteristics of a Metasurface Containing GaN- coated Spherical Inclusions. 17

3.1 Comparison of a Metasurface Containing of Magneto-Dielectric Spherical Inclusions Plots with Holloway Plot (COMSOL).................17

3.2 Comparison of a Metasurface Composed of coated (GaN) Spherical Inclusions Plot with Holloway Plot (COMSOL-Plots)....................21

4 Conculsion **23**

5 Future work **25**

Bibliography **27**

List of Figures

2.1 A metasurface is placed along the z-axis and extends in the yz plane. It consists of regularly arranged spherical scatterers. This metasurface is positioned at the boundary between two distinct media. The medium above the metasurface is referred to as medium 1, and the medium below the metasurface is referred to as medium 2. 9
2.2 Free Space Region (COMSOL) 14
2.3 Magneto-Dielectric Spheres (COMSOL) 14
2.4 Gallium-Nitride Coating (COMSOL) 16

3.1 Plot showing the reflection magnitude of coefficient $|R|$ as a corresponding result of the relative permeability μ_{rp} of the sphere comprising the metasurface. The other values are given in Holloway Citation [1, 2]. The reflection magnitude of the coefficient based upon the theory is in good matching with Fig. 11 of Ref. [1] and Fig. 9 of Ref. [2] 19
3.2 The variation of the reflection coefficient with the permeability, μ_{rp}, of the spherical particles that make up the metasurface 20
3.3 Plot of magnitude of reflection $|R|$ vs relative permeability μ_{rp} 22

Abbreviations

MD	Magnetodielectric
GaN	Gallium Nitride
MS	Meta-Surface
RC	Radi and coworkers
HSFs	Hyper Surfaces
EMS	Electromagnetic Scattering

Chapter 1

Introduction

A meta-surface (MS) is a two-dimensional equivalent of bulk metamaterial [1]. Metamaterials are composed of periodic sub-wavelength metal/dielectric structures that resonantly couple to the electric and/or magnetic components of the incident electromagnetic fields, exhibiting properties that are not found in nature [2] . Meta-surfaces manipulate light by arranging sub-wavelength structures on a surface to control phase, polarization, and amplitude, enabling advanced optics in a compact form [3] . It has historical roots in using patterns for electromagnetic waves and sound control in ancient art and architecture. Today, nanotechnology and material science have propelled metasurface to a new level of capability. It has many applications such as exotic optical phenomena and various useful planar optical devices [4, 5] , Quantum optics, Antenna and Radar, Sensing and Imaging, and Telecommunications.

The electromagnetic metasurfaces are very important due to their many application [6]. Maci and co-workers have introduced the concept of meta-surfacing, i.e., addressing wave on impenetrable metasurfaces . They have developed the meta-surfacing concept using variations in surface impedance and a localized dispersion equation. An analyti-cal framework and metasurface applications were presented by Holloway and co-workers [7]. They observed that metasurfaces require reduced spatial occupancy and exhibit lower losses within the microwave and optics.

A concept of polarization transformer has been studied by Niemi and co-workers [8]. They concentrated on diverse categories of devices for transforming polarization. Alexandra et al. have developed an idea of planar photonics using metasur-faces [9]. Younas et al. have developed the concept of metamirrors [10]. They presented a metasurface composed of thin sheets containing resonant structures with bi-anisotropic scatterers. For their design, they utilized a special type of particle called an omega bi-anisotropic particle. Together, these studies are helping to grow the field of metasurfaces, which are used for making new and useful devices in photonics and changing how light moves.

In a recent survey, Zhao [11] looked at the latest improve- ments in optical meta-surfaces. They described about new ideas in theory, how to model things, and how to experiment with optical metasurfaces. They also discussed the behavior of a periodic array of inclusions in a homogenized metasurface based on the geometry and shape of the inclusions. They also presented about how optical metasurfaces are used for applications like making lenses,beam shaping, and optical communications. In another group, Asadchy and co-workers have introduced functional metamirrors using bianisotropic inclu- sions [12]. They made these mirrors using unique particles and shapes, giving them cool abilities like electricity and magnetism. The authors [13, 14] also talked about interesting ways to use metasurfaces. All of this adds up to lots of exciting progress in the field of metasurfaces, with many practical uses in optics and beyond.

Ding and his team [15] provided a detailed look at the basic concept and use of gradient metasurfaces. These special surfaces change how light behaves across their surface, making the way light moves, its strength, and its direction all change from one place to another place. They discussed about different gra- dient metasurfaces, like ones that control light with their shape, bounce light back, and use the Huygens principle. They also explored various ways gradient metasurfaces are used, such as creating waveplates, flat lenses spiral phase plates, broadband absorbers, color printing, holograms, polarimeters, surface wave couplers, and also nonlinear metasurfaces. They also mentioned how gradient metasurfaces can work for more complex items, not just regular light behavior.

Yazdi and Albooyeh's [16] have extended the normal illumination analysis of the metasurface to the oblique angles of incidence. They mathematically derived the interaction coefficients necessary for a general analysis of metasurfaces. In practice metasurfaces applications, both normal and tangential polarization currents play vital roles. The researcher clarified the significance of these currents when metasurfaces are subjected to oblique illumination. Their proposed formulation was applied to two illustrative cases involving bi-anisotropic metasurfaces crafted from chiral and omega inclusions. Through their study, Yazdi and Albooyeh provided valuable insights into how metasurfaces behave under various angles of light incidents, contributing to the understanding of metasurfaces' performance and enabling more accurate design considerations for real-world applications.

The physics applications of bi-anisotropic metasurfaces have been studied by Asdchy et al [17]. They contended that in general linear metasurfaces, the electric surface current can arise both incident electric and magnetic. Similarly, they noted that external electric fields can also lead to magnetic polarization and magnetic currents. They termed metasurfaces as bi-anisotropic when it shows magneto-electric coupling. This type of metasurface offers immediate applications in precise manipulation of wave fronts using gradients. It has been demonstrated that omega-type bianisotropy is a fundamental requirement for the design of 100% efficient anomalous refractive and reflective metasurfaces.

Wong and Eleftheriades [18] have introduced a new type of metasurface that is able to reflect a knowing incident electromagnetic wave in an arbitrary direction with perfect power efficiency. They introduced bipartite Huygens metasurfaces composed of ground-backed electric dipoles. They verified their proposed design by full-wave simulation and experimental measurement. Notably, their proposed design stands out for its straightforward single-layer structure, making it feasible for practical fabrication even at higher frequency ranges, including millimeters, terahertz, and beyond.

The passage described the study of hypersurfaces (HSFs) conducted by Pitilakis and colleagues [19]. Hyper surfaces are planar metamaterial platforms whose behavior is controlled by software. They serve as a bridge between hardware and software, allowing for programmable control of electromagnetic scattering properties across their surface. The main challenge in de- signing HSFs lies in managing networking between tiles within and across the surfaces, particularly as the frequency of operation increases. Various methods for powering and communication, such as adaptive smart metasurfaces and remotely-powered interactive electromagnetic mantles, are being explored for gateways or chips. These approaches have applications in Internet of Things (IoT) systems.

Radi and co-workers (RC) have introduced the concept of tunable metasurface in [7]. They have given an analytic treatment of tunable metasurface. They talked about making a real version of their theoretical model and how they tested it. They showed that their transparent metasurface can change in special ways. They also made an electronically tunable metasurface which is capable of rotating the polarization of an arbitrarily polarized incident wave without changing its axial ratio. They concluded that a proposed design of polarization rotating can provide real-time manipulation of polarization of communication and radar systems.

Gallium nitride (GaN) and related materials, such as ternary AlGaN and InGaN, as well as quaternary InAlGaN, have found applications in optoelectronic components. The synthesis of the first poly-crystalline GaN material dates back to 1932 [20]. Studies on the crystal structure of GaN have been conducted on GaN powders [21]. GaN-based high-frequency (HF) performance has been explored in high-electron-mobility transistors (HEMTs) [22], with Panasonic and Infineon producing the first fully industrial-qualified ”true” normally-off devices [23], which have gained traction in the industry. To further expand upon this, the utilization of GaN and its derivatives has significantly impacted the field of optoelectronics, paving the way for advancements in high-frequency performance and reliability. Moving forward, the ongoing exploration of these materials holds promise for even more groundbreaking advancements in optoelectronics and related industries.

In this work, we explore how a special surface, called a Metasurface, reflects light under oblique incidence. We are studying a symmetrical metasurface composed of a periodic arrangement of dipole scatterers. We take two approaches. One is uncoated magneto-dielectric (MD) and the other is Gallium Nitride (GaN) coated spherical inclusions. GaN is a good conductor and shows conductive behavior. Our goal is to carefully study and understand how these materials work together to absorb light. By using theoretical analysis and software, we study how electromagnetic waves behave when they are incident to a metasurface composed of spherical inclusion. Through this work, we not only enhanced our understanding of symmetrical metasurfaces containing uncoated and coated magneto-dielectric spherical inclusions but also made valuable contributions, to the field of electromagnetic and metasurfaces for future developments. .

1.1 Layout

The work presented in this dissertation follows the layout presented below.

1.1.1 Chapter 2

In this chapter, we will discuss the geometry and derivation of the absorption characteristics of a meta-surface consisting of spherical inclusions with coating and without coating cases. We will also provide complete details of the calculations and geometric information.

1.1.2 Chapter 3

In this chapter, we will discuss the analysis of the absorption characteristics of a meta-surface consisting of spherical inclusions as coated (GaN) and without coated (MD spherical inclusions using COMSOL plots. We will compare the characteristics of a meta-surface consisting of spherical inclusions as coated (GaN) and without coated (MD) spherical inclusions with Holloway plots, by generating these plots through a COMSOL. Additionally, we will analyze the comparison of a metasurface composed of coated (GaN) spherical inclusions with Holloway plots using COMSOL software.

1.1.3 Chapter 4

In this chapter, we conclude the entire thesis by providing a comprehensive report detailing the entirety of the work conducted throughout my research.

1.1.4 Chapter 5

In this chapter, we will discuss the future prospects of our work. Furthermore, we will explore the benefits, potential applications, and significance in electromagneticS.

Chapter 2

Geometry and Derivation of Absorption Characteristics for a Metasurface Comprising Coated (GaN) Spherical Inclusions

In this section, we explore the geometric and mathematical foundations underlying the electromagnetic behavior of a metasurface containing spherical inclusions. Our work is specifically focused on metasurfaces that are composed of both uncoated Magneto-Dielectric (MD) and Gallium Nitride (GaN) coated Magneto-Dielectric (MD) spherical particles. The primary aim is to study the electromagnetic properties of these metasurfaces by investigating their interaction with incident electromagnetic waves. Through a comprehensive mathematical derivation, we seek to provide a deeper understanding of how the arrangement and composition of the spherical inclusions influence the reflection of electromagnetic waves. Our analysis involves a comparative study of uncoated MD particles and GaN-coated spheres, with the goal of uncovering the unique effects that different materials and configurations impose on the metasurface's response to electromagnetic radiation. This endeavor contributes not only to the advancement of theoretical knowledge surrounding metasurfaces but also establishes a foundation for potential practical applications. These applications span a wide array of fields, ranging from optics and telecommunications to sensing, offering promising prospects for advanced wave manipulation and control.

2.1 Mathematical Derivation

It is assumed that a metasurface is composed of a periodic arrangement of inclusion in the yz-plane, with uniform spacing denoted as 'd' along both the y-axis and z-axis respectively. It is considered that a unit vector $\hat{n}$ is normal to the plane of the metasurface(MS). In our problem, this metasurface (MS) is positioned at the coordinate $x = 0$. It is assumed that the region where $x > 0$ is occupied by Medium 1. A medium 1 is characterized by a propagation constant $k_1 = k_o\sqrt{\mu_{r1}\varepsilon_{r1}}$, where its intrinsic impedance is $\eta_1 = \eta_0\sqrt{\frac{\mu_{r1}}{\varepsilon_{r1}}}$. The parameters η_0 and k_o represent the intrinsic impudence and wave number of free space respectively. It is also assumed that $x < 0$ is occupied by Medium 2. A medium 2 is characterized by a propagation constant $k_2 = k_o\sqrt{\mu_{r2}\varepsilon_{r2}}$, where its intrinsic impedance is $\eta_2 = \eta_0\sqrt{\frac{\mu_{r2}}{\varepsilon_{r2}}}$ respectively.

The electric and magnetic fields tangential to the surface are denoted as $Et1$ and $Ht1$ within medium 1, as provided below.

$$E_{t1} = E_i e^{-jk_1 \sin\theta_i z} + r_{TE} E_i e^{-jk_1 \sin\theta_i z} \tag{2.1}$$

and for magnetic fields tangential can be written as

$$n \times \mathbf{H}_{t1} = \frac{E_i}{\eta_1}\cos\theta_i e^{-jk_1 \sin\theta_i z} - r_{\text{TE}}\cos\theta_r \frac{E_i}{\eta_1} e^{-jk_1 \sin\theta_i z} \tag{2.2}$$

where n is unit normal vector to MS plane and r_{TE} is complex reflection respectively. But where θ_i and θ_r are taken to be the angles of incidence and reflection, respectively.

The electric and magnetic fields tangential to the surface are denoted as $Et2$

and $Ht2$ within medium 2, as provided below.

$$E_{t1} = r_{TE} E_i e^{-jk_1 \sin\theta_i z} \tag{2.3}$$

$$n \times \mathbf{H}_{t2} = r_{\mathrm{TE}} \frac{E_i}{\eta_2} \cos\theta_t e^{-jk_2 \sin\theta_i z} \tag{2.4}$$

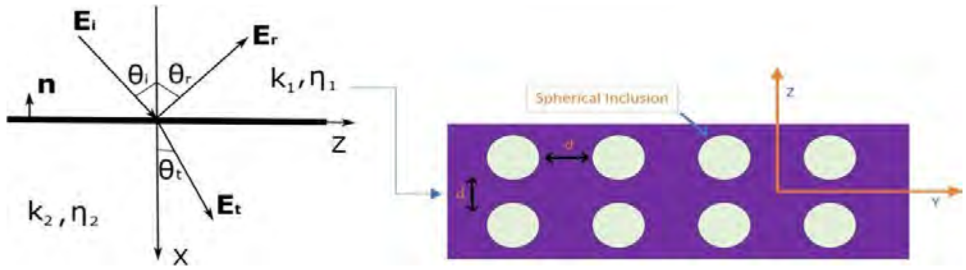

Figure 2.1: A metasurface is placed along the z-axis and extends in the yz plane. It consists of regularly arranged spherical scatterers. This metasurface is positioned at the boundary between two distinct media. The medium above the metasurface is referred to as medium 1, and the medium below the metasurface is referred to as medium 2.

Where t_{TE} is the complex transmission coefficient, and θ_t is the angle of reflection. The tangential field boundary conditions at the metasurface plane are provided below[16].

$$E_{t1} - E_{t2} = A_1 E_i e^{-jk_1 \sin\theta_i z} \tag{2.5}$$

$$n \times H_{t1} - n \times H_{t2} = B_1 E_i e^{-jk_1 \sin\theta_i z} \tag{2.6}$$

$$A_1 = \frac{j\omega}{A_d} \left(\hat{\alpha}^{zy}_{me} + \hat{\alpha}^{zz}_{mm} \frac{\cos\theta_i}{\eta_1} \right) \tag{2.7}$$

$$B_1 = \frac{j\omega}{A_d} \left(\hat{\alpha}^{yy}_{ee} + \hat{\alpha}^{yz}_{em} \frac{\cos\theta_i}{\eta_1} \right) \tag{2.8}$$

where $A_d = d^2$. These combined polarizabilities also include the effects of interaction within the metasurface plane. Just like, $\hat{\alpha}^{yy}_{ee}$, $\hat{\alpha}^{zz}_{mm}$, $\hat{\alpha}^{yz}_{em}$ and $\hat{\alpha}^{zy}_{me}$ are collective electric, magnetic, magneto-electric and electromagnetic polarizabilities. By replacing Equations (1) to (4) with Equations (5) to (6) and performing some calculations, we can determine the complex reflection as follows,

$$r_{TE} = R = \frac{\eta_1\eta_2}{\eta_1 \cos\theta_t + \eta_2 \cos\theta_r} \frac{\cos\theta_i}{\eta} - \frac{\cos\theta_t}{\eta_c}(1 - A_1) - B_1 \qquad (2.9)$$

The values of A_1 and B_1 are provided in equations (2.7) and (2.8) given above.

To make the analysis simpler, it is assumed that the meta-surface consists of spherical inclusions as coated (GaN) and without coated (MD) spherical inclusions. An uncoated sphere is simply made up of magneto-dielectric material, while a coated sphere is made up of a gallium nitride coating on the outside, which is still composed of magneto-dielectric material. In the case in which inclusions are without coating, the radius is denoted as $'a,'$ with ${}_r$ showing the relative permittivity and r showing the relative permeability of the inclusion. In the case of GaN-coated inclusions, the inside core has a radius of a1, while the outer shell has a radius of a.

In this scenario, the internal shell has relative permittivity ε_r and relative permeability μ_r, while the outer region material is characterized by relative parameters ε_{rc} and μ_{rc}. The wave numbers in the internal shell and outer regions are determined as $k = k_o(\mu_r\varepsilon_r)^{1/2}$ for the core and $k_c = k_o(\mu_{rc}\varepsilon_{rc})^{1/2}$ for the shell. Within this metasurface, the two types of spherical inclusions, with and without coating, exhibit no cross-coupling. This means that there is no interaction or coupling between electromagnetic and magneto-electric properties.

That's way

$$\hat{\alpha}^{yz}_{em} = \hat{\alpha}^{zy}_{me} = 0. \qquad (2.10)$$

The combined electric and magnetic polarizabilities, namely $\hat{\alpha}^{yy}_{ee}$ and $\hat{\alpha}^{zz}_{mm}$, depend on the individual polarizabilities α_{ee}^{yy} and α_{mm}^{zz}, as well as the interactions within the metasurface plane[8, 16]. The individual electric and magnetic polarizabilities α_{ee}^{yy} and α_{mm}^{zz} of uncoated or coated spheres can be expressed as[24].

$$\alpha_{ee}^{yy} = j\frac{6\pi\varepsilon_0 b_1^{sc}}{k_o^3}, \quad \alpha_{mm}^{zz} = j\frac{6\pi\mu_0 a_1^{sc}}{k_o^3} \tag{2.11}$$

We will apply equation(2.9) for two types of spherical inclusions, i.e., with and without coating inclusions comprising of a metasurface. The unit cell polarizability for uncoated and coated spheres can be found from electric polarizability tensor[24] as,

$$\hat{\bar{\alpha}}_{ee} = \left[\bar{I}_t - \bar{\alpha}_{ee}\cdot\bar{\beta}_e - \bar{\alpha}_{em}\cdot\bar{\beta}_m\cdot\left(\bar{I}_t - \bar{\alpha}_{em}\cdot\bar{\beta}_m\right)^{-1}\cdot\bar{\alpha}_{me}\cdot\bar{\beta}_e\right]^{-1}\cdot\left[\bar{\alpha}_{ee} + \bar{\alpha}_{em}\cdot\bar{\beta}_m\cdot\left(\bar{I}_t - \bar{\alpha}_{em}\cdot\bar{\beta}_m\right)^{-1}\cdot\bar{\alpha}_{me}\right] \tag{2.12}$$

In case of sphere,we substitute $\bar{\alpha}_{me} = \bar{\alpha}_{em} = 0$ in Eq.(2.12) to get

$$\hat{\bar{\alpha}}_{ee} = \left(\bar{I}_t - \bar{\alpha}_{ee}\cdot\bar{\beta}_e\right)^{-1}\cdot\bar{\alpha}_{ee} \tag{2.13}$$

Where $\bar{I}_t$, $\bar{\alpha}_{ee}$ and $\bar{\beta}_e$ are given below as

$$\bar{I}_t = \begin{bmatrix} 1 & 0 \\ 0 & 1 \end{bmatrix},$$
$$\bar{\alpha}_{ee} = \begin{bmatrix} 1 & 0 \\ 0 & 1 \end{bmatrix},$$
$$\bar{\beta}_e = \begin{bmatrix} \beta_e & 0 \\ 0 & \beta_e \end{bmatrix}$$

Thus from Eqs.(2.13)-(2.12),we obtain collective electric polarizability $\hat{\alpha}_{ee}^{yy}$ as,

$$\hat{\alpha}_{ee}^{yy} = \frac{1}{(\alpha_{ee}^{yy})^{-1} - \bar{\beta}_e} \tag{2.14}$$

where $\hat{\alpha}^{yy}_{ee}$ is scalar electric individual polarizaibilty. The individual electric

polarizibility $\hat{\alpha}^{yy}_{ee}$ for a spherical scatter can be written as

$$\hat{\alpha}^{yy}_{ee} = j\frac{6\pi\varepsilon_o b^{sc}_1}{k_o^3} \tag{2.15}$$

Here b^{sc}_1 is dipolar Mie scattering coefficient of electric type. Likewise the unit magnetic cell collective tensor is given by[24],

$$\bar{\alpha}_{ee} = \left[\bar{I}_t - \bar{\alpha}_{mm}\cdot\bar{\beta}_m - \bar{\alpha}_{me}\cdot\bar{\beta}_e\cdot\left(\bar{I}_t - \bar{\alpha}_{ee}\cdot\bar{\beta}_e\right)^{-1}\cdot\bar{\alpha}_{em}\cdot\bar{\beta}_m\right]^{-1}\cdot\left[\bar{\alpha}_{mm} + \bar{\alpha}_{me}\cdot\bar{\beta}_e\cdot\left(\bar{I}_t - \bar{\alpha}_{ee}\cdot\bar{\beta}_e\right)^{-1}\cdot\bar{\alpha}_{em}\right] \tag{2.16}$$

putting $\bar{\alpha}_{em} = \bar{\alpha}_{me} = 0$ in Eq(2.16),we get,

$$\bar{\alpha}_{mm} = \left(\bar{I}_t - \bar{\alpha}_{mm}\cdot\bar{\beta}_m\right)^{-1}\cdot\bar{\alpha}_{mm} \tag{2.17}$$

where $\bar{\alpha}_{mm}$ and $\bar{\beta}_m$ are given as,

$$\bar{\alpha}_{mm} = \begin{bmatrix} 0 & 0 \\ 0 & \alpha_{mm} \end{bmatrix}, \tag{2.18}$$

$$\bar{\beta}_m = \begin{bmatrix} \frac{\beta_e}{\eta_0^2} & 0 \\ 0 & \frac{\beta_e}{\eta_0^2} \end{bmatrix} \tag{2.19}$$

So putting Eq.(2.19.2.18) in Eq.(2.17) and solving it we get,

$$\hat{\alpha}^{zz}_{mm} = \frac{1}{(\alpha^{zz}_{mm})^{-1} - \bar{\beta}_m} \tag{2.20}$$

Where $\hat{\alpha}^{zz}_{mm}$ is scalar individual magnetic polarizability. For a spherical spherical scatter, it can be written as[24].

$$\hat{\alpha}^{zz}_{mm} = j\frac{6\pi\varepsilon_0 a^{sc}_1}{k_0^3} \tag{2.21}$$

2.1.1 Uncoated Spherical Scatters

Uncoated spherical inclusions are made up of MD material, which has the relative permittivity ε_{rp} of 13.8 - j0.1 and relative permeability μ_{rp} as 11. Its relative permittivity ε_{rp} is different from unity which is why it is known as magneto-dielectric. The relative permeability μ_{rp} values vary from 0 to 100 to study the reflection characteristics. Here a^{sc}_1 is the dipolar Mie scattering coefficient of magnetic type. For uncoated spherical scatters, the coefficient a^{sc}_1 and b^{sc}_1 are given as,

$$b^{sc}_1 = \frac{\mu_{r1}\, j_1(\rho_{11})[\rho_1(\rho_{11})]' - (\mu_{r1}\varepsilon_{r1}) j_1(\rho_{11})[\rho_1\, j_1(\rho_1)]'}{\mu_{r1} h^{(1)}_1(\rho_{11})[\rho_1\, j_1(\rho_{11})]' - (\mu_{r1}\varepsilon_{r1})(\rho_{11})[\rho_1 h^{(1)}_1(\rho_1)]'} \tag{2.22}$$

$$a^{sc}_1 = -\frac{\mu_{r1} j_1(\rho_{11})[\rho_1(\rho_1)]' - (j_1(\rho_1)[\rho_1 j_1(\rho_{11})]')}{\mu_{r1} j_1(\rho_{11})[\rho_1 h^{(1)}_1(\rho_1)]' - h^{(1)}_1(\rho_1)[\rho_{11} j_1(\rho_{11})]'} \tag{2.23}$$

Here, the functions $j_1(\cdot)$ and $h^{(1)}_1(\cdot)$ represent the spherical Bessel and spherical Hankel functions with order one, respectively. The values ρ_1 and ρ_{11} have the following meanings

$$\rho_1 = k_0 a_1, \quad \rho_{11} = k_1 a_1, \quad k_1 = k_0 = (\mu_{r1}\varepsilon_{r1})^{1/2} \tag{2.24}$$

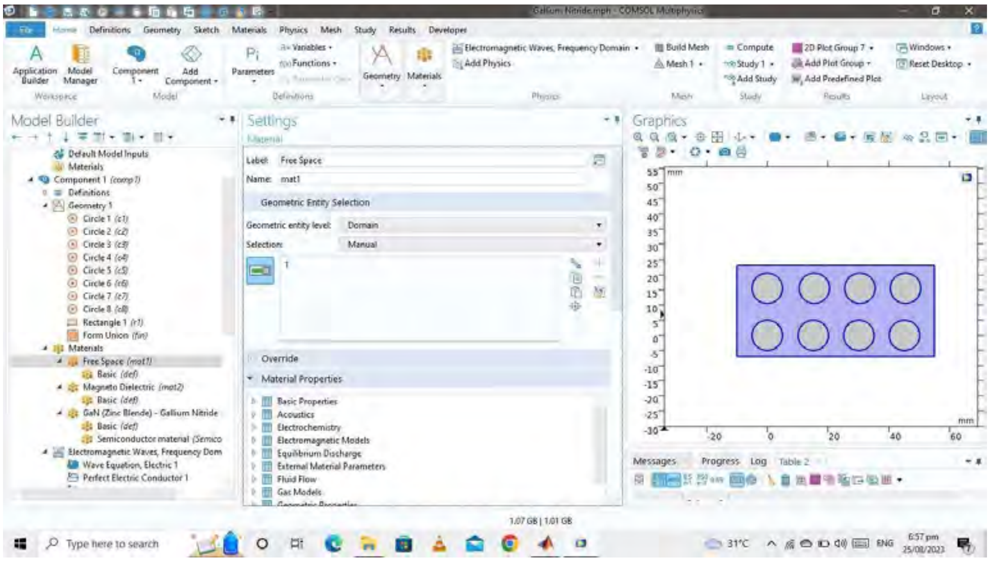

Figure 2.2: Free Space Region (COMSOL)

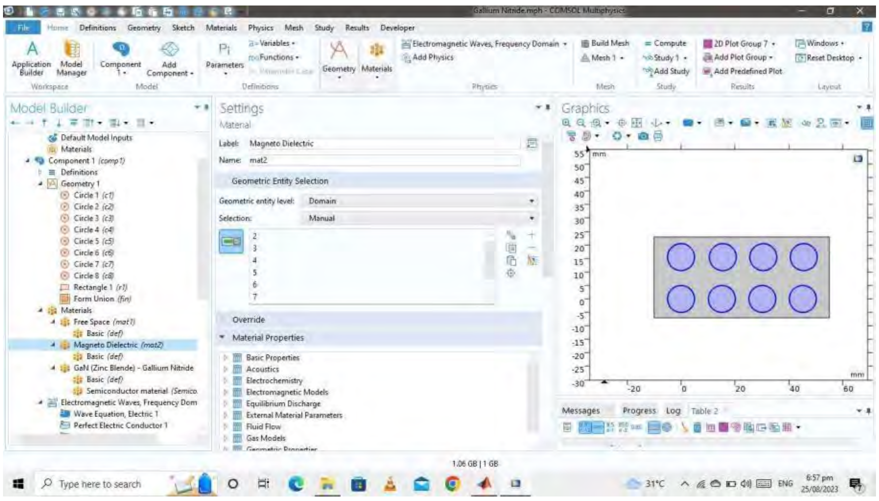

Figure 2.3: Magneto-Dielectric Spheres (COMSOL)

2.1.2 Coated Spherical Scatters

Gallium Nitride is used for coating MD spherical inclusions which has a relative permittivity μ_{rp} of 8.9. Similarly, as for the uncoated scenario, relative permeability μ_{rp} values vary from 0 to 100 to study the reflection characteristics. For the case of coated spherical scatters, the scattering coefficients a_1^{sc}, b_1^{sc} become as

$$b_1^{sc} = -\frac{\left(\frac{1}{\varepsilon_{r2}}\right) j_1(\rho_0) A_\varepsilon - [\rho_0 j_1(\rho_0)]' B_\varepsilon}{\left(\frac{1}{\varepsilon_r}\right) h_1^1(\rho_0) A_\varepsilon - [\rho_0 h_1^1(\rho_0)]' B_\varepsilon} \tag{2.25}$$

$$a_1^{sc} = -\frac{\left(\frac{1}{\mu_{r2}}\right) j_1(\rho_0) A_\mu - [\rho_0 j_1(\rho_0)]' B_\mu}{\frac{1}{\mu_{r2}} h_1^1(\rho_0) A_\mu - [\rho_0 h^1(\rho_0)]' B_\mu} \tag{2.26}$$

$$A_\varepsilon = \frac{j_1(\rho_{11})}{\varepsilon_{r2}} G1 + \frac{[\rho_{11} j_1(\rho_{11})]'}{r1} G2 \tag{2.27}$$

$$B_\varepsilon = \frac{j_1(\rho_{21})}{\varepsilon_{r2}} G3 + \frac{[\rho_{11} j_1(\rho_1 1)]'}{\varepsilon_{r1}} G4 \tag{2.28}$$

$$A_\mu = \frac{j_1(\rho_{11})}{\mu_{r2}} G1 + \frac{[\rho\ j]'}{\mu_{r1}} G2 \tag{2.29}$$

$$B_\mu = \frac{j_1(\rho_{11})]}{\mu_{r2}} G3 + \frac{[\rho_{21} j_1(\rho_{11})]'}{\mu_{r1}} G4 \tag{2.30}$$

$$G1 = [\rho_2 j_1(\rho_2)]'[\rho_{21} y_1(\rho_{21})]' - [\rho_{21} y_1(\rho_{21})]'[\rho_2 y_1(\rho_2)]' \tag{2.31}$$

$$G2 = j_1(\rho_{21})[\rho_2 y_1(\rho_2)]' - [\rho_2 j_1'(\rho_2)] y_1(\rho_{21}) \tag{2.32}$$

$$G3 = j_1(\rho_2)[\rho_{21} y_1'(\rho_{21})] - [\rho_{21} j_1'(\rho_{21})] y_1(\rho_2) \tag{2.33}$$

$$G4 = j_1(\rho_{21}) y_1(\rho_2) - j_1(\rho_2) y_1(\rho_{21}) \tag{2.34}$$

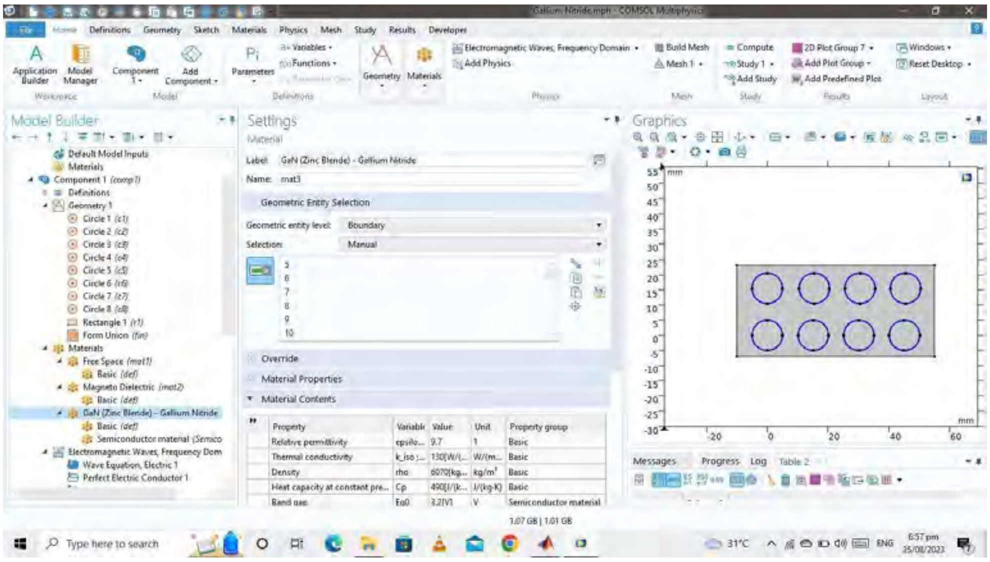

Figure 2.4: Gallium-Nitride Coating (COMSOL)

Where factors $\rho_0, \rho_2, \rho_{21}$ are defined as we can write below

$$\rho_0 = k_0 a, \rho_2 = k_2 a, \rho_{21} = k_2 a_1 \tag{2.35}$$

In this context, the notation $y_1(\cdot)$ represents the spherical Neumann function of order one, and "*primer*" denotes differentiation with respect to the argument of the Bessel function under consideration.

Chapter 3

Analysis of Absorption Characteristics of a Metasurface Containing GaN- coated Spherical Inclusions.

In this chapter, we discuss the comparison of magneto-dielectric materials with Holloway plots, as well as the comparison of Gallium Nitride with Holloway plots.

3.1 Comparison of a Metasurface Containing of Magneto-Dielectric Spherical Inclusions Plots with Holloway Plot (COMSOL)

In this section, we discuss the comparison of the magneto-dielectric material plot with the Holloway plot. To validate the theory introduced in the previous section, we consider a scenario where the medium in the background is taken to be free space, and the metasurface consists of MD inclusions, as described in [1, 2]. The wave for incidence is considered to be normal. Considering an uncoated spherical inclusions with a radius of $a = 5mm$, relative permittivity $\varepsilon_r = 15$, and spacing $d = 10.15mm$, the analysis is performed at a frequency of $1.5GHz$, following the approach adopted by Holloway and coworkers[1, 2]. Applying the formulated approach, we depict the magnitude of the reflection coefficient $|R|$ with respect to the relative permeability μ_{rp} has been shown in Fig.(3.1). This agreement with the reported works validates the proposed theory[25]

In this paragraph, we compare Figure 3.1 with Figure 3.2 and observe how both figures illustrate their respective behaviors. From Figure 3.1, it's evident that the metasurface transitions from total reflection to total transmission as the permeability of the spherical scatterers varies. Notably, complete reflection ($|R| = 1$) occurs at $\mu_{rp} = 46.04$, while total transmission ($|R| = 0$) happens at $\mu_{rp} = 15$.

Additionally, Figure 3.2 demonstrates a similar behavior to Figure 3.1. Both figures depict that at $\mu_{rp} = 0$, the value of $|R|$ is approximately 0.3. Similarly, at $\mu_{rp} = 0$, the value of $|R|$ is 0. At $\mu_{rp} = 56$, the value of $|R|$ is also 0. As we move along the graphs, we observe that at $\mu_{rp} = 71$, the value of $|R|$ is 0.2. Further along, at $\mu_{rp} = 91$, the value of $|R|$ is 0.1. Continuing along the graphs, we see that at $\mu_{rp} = 100$, the value of $|R|$ is approximately 0. This consistent behavior is observed for both figures.

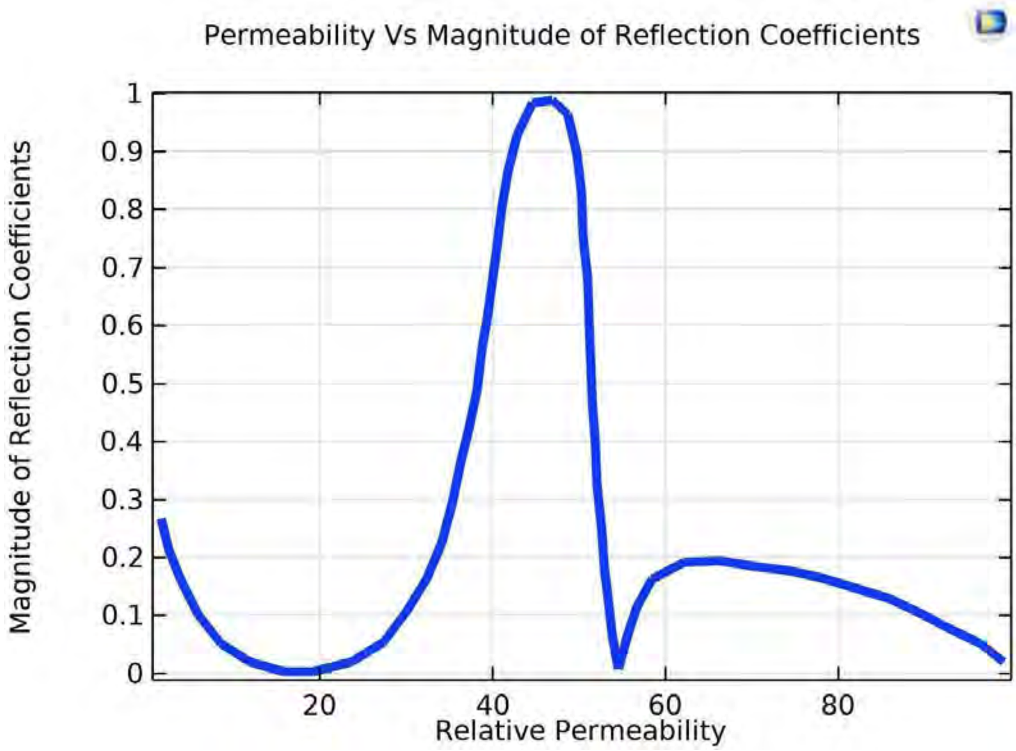

Figure 3.1: Plot showing the reflection magnitude of coefficient $|R|$ as a corresponding result of the relative permeability μ_{rp} of the sphere comprising the metasurface. The other values are given in Holloway Citation [1, 2]. The reflection magnitude of the coefficient based upon the theory is in good matching with Fig. 11 of Ref. [1] and Fig. 9 of Ref. [2]

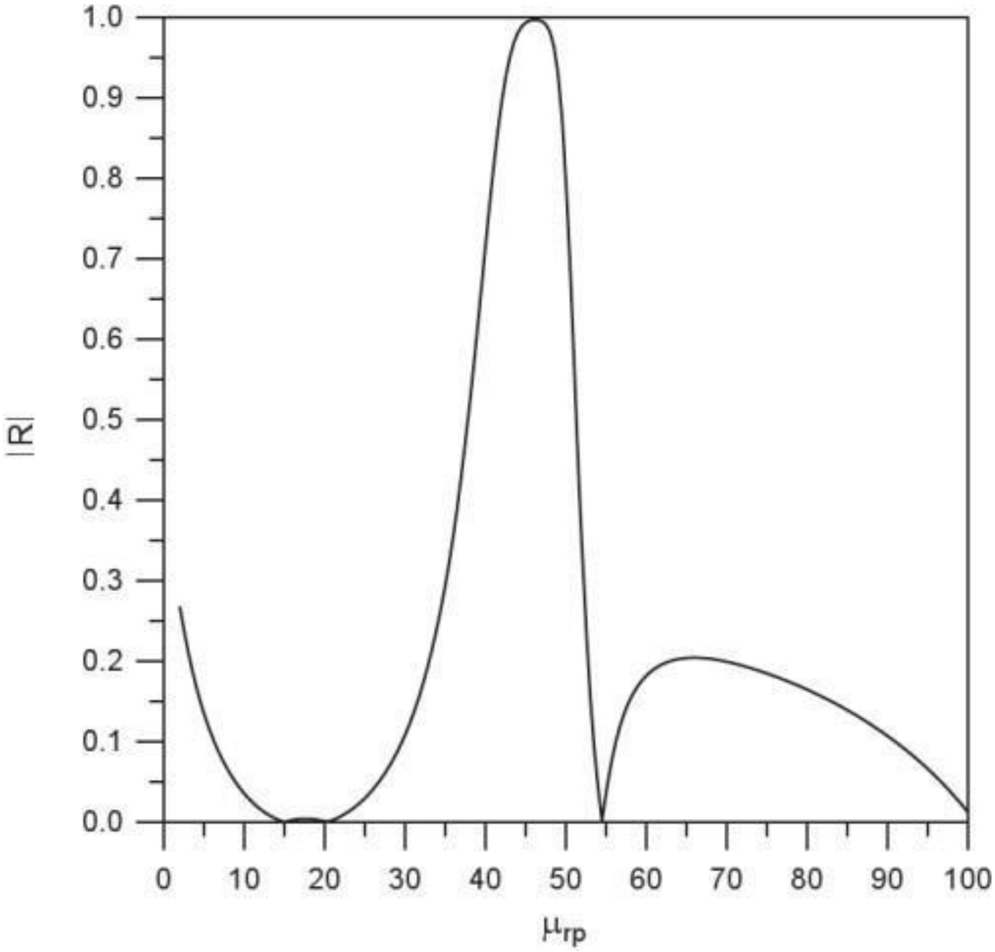

Figure 3.2: The variation of the reflection coefficient with the permeability, μ_{rp}, of the spherical particles that make up the metasurface.

3.2 Comparison of a Metasurface Composed of coated (GaN) Spherical Inclusions Plot with Holloway Plot (COMSOL-Plots)

Here, we compare the figure of a Holloway plot with the plot of a metasurface containing spherical inclusions. Additionally, we examine the scenario where the spherical inclusions are coated with GaN. The wave considered for incidence is taken to be normal. Considering a coated spherical scatterer with a radius of $a = 5mm$, relative permittivity $\varepsilon_r = 15$, and spacing $d = 10.15mm$, the analysis is performed at a frequency of $1.5GHz$, and we take values for free space (because both mediums are taken to be free space) $a_1/d = 0.39$, $\varepsilon_{r1} = \mu_{r1} = 1$, $\varepsilon_{r2} = \mu_{r2} = 1$. Figures 3.3 and 3.2 depict the absorption characteristics of metasurfaces consisting of with and without coated spherical inclusions, respectively. Fig.(3.3) represents the reflection coefficient $|R|$ with the permeability μ_{rp} of GaN-coated MD spheres. It is observed from Figure that $|R| = 0.5$ occurs for $\mu_{rp} = 25$, and $|R| =\approx 1$ occurs for $\mu_{rp} = 35$. Similarly, from the Figure, $|R| = 1$ occurs for $\mu_{rp} = 65$, and $|R| = 0$ occurs for $\mu_{rp} = 78$. Additionally, $|R| = 0$ occurs for $\mu_{rp} = 27$.

We compare Fig. (3.3) and Fig. (3.2). From Fig. (3.2), we observe that $|R| = 0$ occurs for $\mu_{rp} = 20$, while from Fig. (3.3), $|R| = 0$ occurs for $\mu_{rp} = 25$. Additionally, in Fig. (3.3), $|R| = 0.3$ occurs for $\mu_{rp} = 5$, and $|R| = 0.5$ occurs for $\mu_{rp} = 25$. Furthermore, we observe from Fig. (3.3) that $|R| = 1$ occurs for $\mu_{rp} = 35$, and in Fig. (3.2), $|R| = 1$ occurs for $\mu_{rp} = 47$. Also, in Fig. (3.2), $|R| = 0$ occurs for $\mu_{rp} = 100$, and in Fig. (3.3), $|R| = 0$ occurs for $\mu_{rp} = 78$. Finally, $|R| = 0.55$ occurs for $\mu_{rp} = 100$.

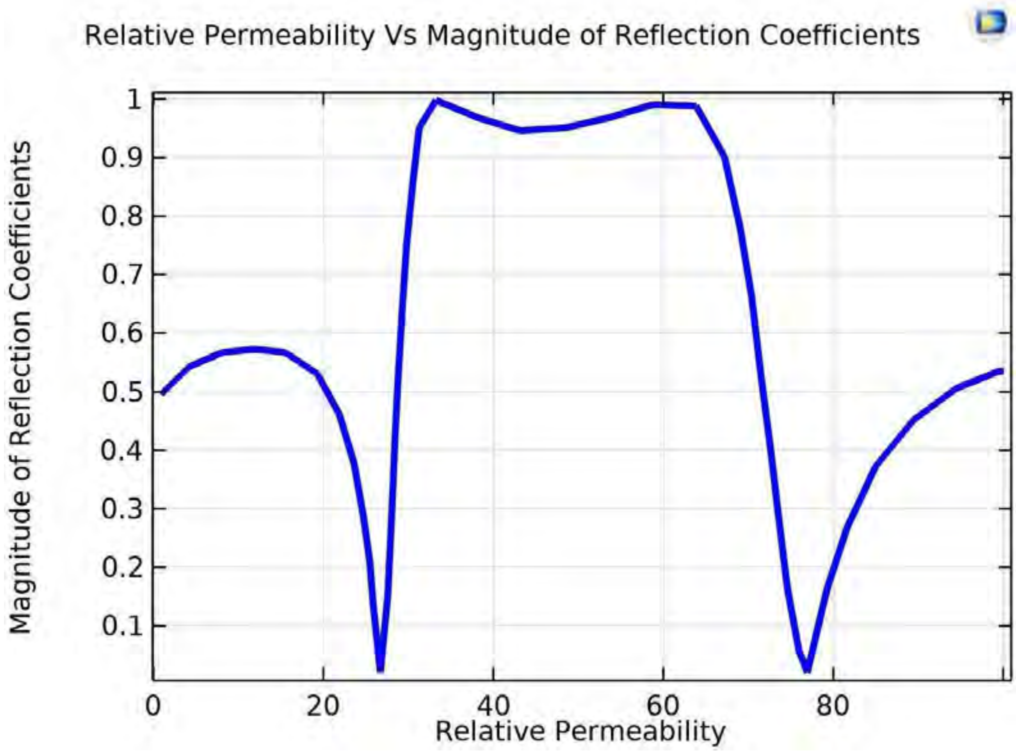

Figure 3.3: Plot of magnitude of reflection $|R|$ vs relative permeability μ_{rp}

From values of relative permeability variating from 0 to 23 , it acts as an absorber and from 23 to 65 it behaves as a good reflector .

Chapter 4

Conculsion

This study shows a comprehensive formulation for understanding the phenomena of absorption and reflection from metasurfaces, especially those composed of an array of uncoated and coated spheres. This endeavor was not merely theoretical; rather, it brought to light practical applications involving real-world materials, magneto-dielectric (MD) substances, and Gallium Nitride (GaN). Magneto-dielectric materials possess a unique combination of magnetic and dielectric properties, allowing for fine-tuning of electromagnetic responses. Gallium Nitride has gained considerable attention due to its exceptional electronic and optical properties. When integrated into metasurfaces, Gallium Nitride opens up possibilities for active control of electromagnetic waves.

The work specifically focused on two areas within the metasurface, one described by μ_2 and k_1, and the other by μ_2 and k_2. The spherical inclusion is made up of Magneto-Dielectric while the coating material is Gallium-Nitride. The normal wave is taken for incidence and free space background is taken for metasurface. For completeness, the individual electric and magnetic polarizabilities are also discussed as well the the magnitude of reflection coefficients is discussed. Using Gallium Nitride coated spherical inclusions in metasurfaces enhances the reflection allowing it to be used as a reflector. GaN is a good conductor because its coefficient of reflection is equal to 1. GaN demonstrates conductive behavior, making it a good conductor and an effective reflector. When integrated into Metasurfaces, Gallium Nitride opens up possibilities for active control of electromagnetic waves.

This study reveals a fascinating insight into how materials and metasur - faces can make a big difference in electromagnetic characteristics. By changing the coating thickness and material, we have shown that we can control how reflection characteristics. This work could bring about major changes in how we design and improve metasurfaces for various uses like changing the direction of waves and adjusting polarization. This research is a blend of theory and real-world applications. By studying materials like magneto-dielectric and Gallium Nitride, we make sure that our findings are useful in today's world.

This research work is dedicated to understanding the characteristics of these materials. By analyzing their properties we open up possibilities for improving technology. This exploration has the potential to bring about advancements in electromagnetism, metasurfaces, and metamaterials. With each finding, we get closer to fully harnessing the capabilities of these materials, in real-life applications that inspire humanity.

Chapter 5

Future work

Our future endeavors in the realm of metasurfaces focus on two key directions. Firstly, we will explore metasurface behavior in various background media, aiming to understand their reflection responses in diverse electromagnetic environments. This will enhance their adaptability to real-world scenarios. Secondly, we will investigate the impact of incident angles on metasurfaces made of uncoated and coated spheres, leading to improved functionality in applications like beam steering and wavefront control. Incorporating MD and GaN materials into metasurfaces holds promise for transformative advancements in technology, such as high-frequency communications and imaging. Our commitment remains steadfast in uncovering new insights and contributing to the field of electromagnetic wave manipulation. This helped us understand better how things scatter and interact within the metasurface. This new understanding is like a strong base for us to explore the bigger effects of our research.

The beauty of my work can be explained throughout all my research. Thus, I assert that this work can be further extended, exploring various types of metasurfaces that can be created using Galium Nitride and other metamaterial dielectric materials. There have been improvements in various aspects, which distinguish and provide unique characteristics to these structures. While we have covered a lot in our current work, there is still so much to explore. We need to look at how different backgrounds and different materials affect this reflection. There is a need to understand how different angles of the incoming waves affect this behavior for both metasurfaces made of spheres with and without coatings.

Looking forward, there is a lot more to discover, and that's exciting. We are driven to learn more about these cool electromagnetic systems and keep contributing to the field of metasurfaces.

Bibliography

[1] Christopher L Holloway, Mohamed A Mohamed, Edward F Kuester, and Andrew Dienstfrey. Reflection and transmission properties of a metafilm: With an application to a controllable surface composed of resonant particles. *IEEE Transactions on Electromagnetic Compatibility*, 47(4):853–865, 2005.

[2] Christopher L Holloway, Edward F Kuester, Joshua A Gordon, John O'Hara, Jim Booth, and David R Smith. An overview of the theory and applications of metasurfaces: The two-dimensional equivalents of metamaterials. *IEEE antennas and propagation magazine*, 54(2):10–35, 2012.

[3] Hou-Tong Chen, Antoinette J Taylor, and Nanfang Yu. A review of metasurfaces: physics and applications. *Reports on progress in physics*, 79(7):076401, 2016.

[4] Nanfang Yu and Federico Capasso. Flat optics with designer metasurfaces. *Nature materials*, 13(2):139–150, 2014.

[5] Hui-Hsin Hsiao, Cheng Hung Chu, and Din Ping Tsai. Fundamentals and applications of metasurfaces. *Small Methods*, 1(4):1600064, 2017.

[6] Stefano Maci, Gabriele Minatti, Massimiliano Casaletti, and Marko Bosiljevac. Metasurfing: Addressing waves on impenetrable metasurfaces. *IEEE Antennas and Wireless Propagation Letters*, 10:1499–1502, 2011.

[7] Zhanni Wu, Younes Ra'di, and Anthony Grbic. Tunable metasurfaces: A polarization rotator design. *Physical Review X*, 9(1):011036, 2019.

[8] Teemu Niemi, Antti O Karilainen, and Sergei A Tretyakov. Synthesis of polarization transformers. *IEEE Transactions on Antennas and Propagation*, 61(6):3102–3111, 2013.

[9] Alexander V Kildishev, Alexandra Boltasseva, and Vladimir M Shalaev. Planar photonics with metasurfaces. *Science*, 339(6125):1232009, 2013.

[10] Younes Ra'di, Viktar S Asadchy, and Sergei A Tretyakov. Tailoring reflections from thin composite metamirrors. *IEEE transactions on antennas and propagation*, 62(7):3749–3760, 2014.

[11] Yang Zhao, Xing-Xiang Liu, and Andrea Alù. Recent advances on optical metasurfaces. *Journal of Optics*, 16(12):123001, 2014.

[12] Viktar S Asadchy, Y Ra'Di, J Vehmas, and SA Tretyakov. Functional metamirrors using bianisotropic elements. *Physical review letters*, 114(9):095503, 2015.

[13] Stanislav B Glybovski, Sergei A Tretyakov, Pavel A Belov, Yuri S Kivshar, and Constantin R Simovski. Metasurfaces: From microwaves to visible. *Physics reports*, 634:1–72, 2016.

[14] VS Asadchy, Ana D´ıaz-Rubio, SN Tcvetkova, D-H Kwon, Amr Elsakka, Mohamed Albooyeh, and SA Tretyakov. Flat engineered multichannel reflectors. *Physical Review X*, 7(3):031046, 2017.

[15] Fei Ding, Anders Pors, and Sergey I Bozhevolnyi. Gradient metasurfaces: a review of fundamentals and applications. *Reports on Progress in Physics*, 81(2):026401, 2017.

[16] Mohammad Yazdi and Mohammad Albooyeh. Analysis of metasurfaces at oblique incidence. *IEEE Transactions on Antennas and Propagation*, 65(5):2397–2404, 2017.

[17] Viktar S Asadchy, Ana D´ıaz-Rubio, and Sergei A Tretyakov. Bianisotropic metasurfaces: physics and applications. *Nanophotonics*, 7(6):1069–1094, 2018.

[18] Alex MH Wong and George V Eleftheriades. Perfect anomalous reflection with a bipartite huygens' metasurface. *Physical Review X*, 8(1):011036, 2018.

[19] Alexandros Pitilakis, Anna C Tasolamprou, Christos Liaskos, Fu Liu, Odysseas Tsilipakos, Xuchen Wang, Mohammad Sajjad Mirmoosa, Kypros Kossifos, Julius Georgiou, Andreas Pitsilides, et al. Software-defined metasurface paradigm: Concept, challenges, prospects. In *2018 12th International Congress on Artificial Materials for Novel Wave Phenomena (Metamaterials)*, pages 483–485. IEEE, 2018.

[20] Warren C Johnson, JB Parson, and MC Crew. Nitrogen compounds of gallium. iii. *The journal of physical chemistry*, 36(10):2651–2654, 2002.

[21] Robert Juza and Harry Hahn. Über die kristallstrukturen von cu3n, gan und inn metallamide und metallnitride. *Zeitschrift für anorganische und allgemeine Chemie*, 239(3):282–287, 1938.

[22] Keisuke Shinohara, Dean C Regan, Yan Tang, Andrea L Corrion, David F Brown, Joel C Wong, John F Robinson, Helen H Fung, Adele Schmitz, Thomas C Oh, et al. Scaling of gan hemts and schottky diodes for submillimeter-wave mmic applications. *IEEE Transactions on Electron Devices*, 60(10):2982–2996, 2013.

[23] Kenichiro Tanaka, Tatsuo Morita, Masahiro Ishida, Tsuguyasu Hatsuda, Tetsuzo Ueda, Kazuki Yokoyama, Ayanori Ikoshi, Masahiro Hikita, Masahiro Toki, Manabu Yanagihara, et al. Reliability of hybrid-drain-embedded gate injection transistor. In *2017 IEEE International Reliability Physics Symposium (IRPS)*, pages 4B–2. IEEE, 2017.

[24] ZA Awan. Nonlocal effective parameters of a coated sphere medium. *Journal of Modern Optics*, 62(7):528–535, 2015.

[25] Zikria Ahmad, ZA Awan, and Arshad Hussain. Electromagnetic characteristics of a metasurface composed of uncoated and coated spherical particles. *Optik*, 220:165103, 2020.